Field ionization of high-Rydberg fragments produced after inner-shell photoexcitation and photoionization of the methane molecule

Kivimaki, A.; Sankari, Anna; Kettunen, J. A.; Stråhlman, Christian; Ruiz, J. Alvarez; Richter, R.

Published in:
Journal of Chemical Physics

DOI:
10.1063/1.4931105

2015

Document Version:
Publisher's PDF, also known as Version of record

Field ionization of high-Rydberg fragments produced after inner-shell photoexcitation and photoionization of the methane molecule

A. Kivimäki,[1,a)] A. Sankari,[2] J. A. Kettunen,[3] C. Stråhlman,[4] J. Álvarez Ruiz,[5] and R. Richter[6]

[1]*Consiglio Nazionale delle Ricerche–Istituto Officina dei Materiali, Laboratorio TASC, 34149 Trieste, Italy*
[2]*Department of Physics, Lund University, P.O. Box 118, 22100 Lund, Sweden*
[3]*Department of Physics, University of Oulu, P.O. Box 3000, 90014 Oulu, Finland*
[4]*MAX IV Laboratory, Lund University, P.O. Box 118, 22100 Lund, Sweden*
[5]*Colegio Los Naranjos, Fuenlabrada, 28941 Madrid, Spain*
[6]*Elettra-Sincrotrone Trieste, Area Science Park Basovizza, 34149 Trieste, Italy*

(Received 9 June 2015; accepted 3 September 2015; published online 17 September 2015)

We have studied the production of neutral high-Rydberg (HR) fragments from the CH_4 molecule at the C 1s → 3p excitation and at the C 1s ionization threshold. Neutral fragments in HR states were ionized using a pulsed electric field and the resulting ions were mass-analyzed using an ion time-of-flight spectrometer. The atomic fragments C(HR) and H(HR) dominated the spectra, but molecular fragments CH_x(HR), x = 1-3, and H_2(HR) were also observed. The production of HR fragments is attributed to dissociation of CH_4^+ and CH_4^{2+} ions in HR states. Just above the C 1s ionization threshold, such molecular ionic states are created when the C 1s photoelectron is recaptured after single or double Auger decay. Similar HR states may be reached directly following resonant Auger decay at the C 1s → 3p resonance. The energies and geometries of the parent and fragment ions have been calculated in order to gain insight into relevant dissociation pathways. © *2015 AIP Publishing LLC.* [http://dx.doi.org/10.1063/1.4931105]

I. INTRODUCTION

A small molecule like CH_4 usually fragments if one of its inner-shell (or core) electrons is promoted to an unoccupied molecular or Rydberg orbital or is completely removed from the molecule. This is because electronic states with an inner-shell hole are highly excited, and typically decay through Auger transitions, where one valence electron fills the core hole and another valence electron is emitted. Resulting electronic states with two holes in valence orbitals are unstable in most molecules; for instance, stable or metastable CH_4^{2+} cations have not been observed.[1] The energy needed to induce inner-shell electron transitions can be delivered by charged particles such as electrons and fast ions or by soft x-ray photons. Since in an x-ray photoabsorption process a photon loses all its energy to the molecule, this excitation method allows one to prepare core-excited molecules in well-defined electronic states and to study their subsequent fragmentation in more detail.

The electron configuration of the methane molecule in the ground state is $1a_1^2\,2a_1^2\,1t_2^6$, where the $1a_1$ orbital derives from the atomic C 1s orbital. Fragmentation of methane has been the subject of numerous studies in both the valence and core-level regions.[2] The Auger spectrum of methane measured just above the C 1s ionization potential (IP) shows three broad features which have been attributed to the $2a_1^{-2}$, $2a_1^{-1}\,1t_2^{-1}$, and $1t_2^{-2}$ final states in the order of increasing kinetic energy and intensity.[3,4] The fragmentation of these final states to positively charged fragments has been studied using Auger electron-ion coincidence spectroscopy by Kukk *et al.*[5] and Auger electron-ion-ion coincidence spectroscopy by Flammini *et al.*[6]

The observed pairs of ionic fragments[6] imply that also neutral fragments are created in dissociation of CH_4^{2+} ions. Their detection is usually more difficult than of the charged fragments. However, if neutral fragments are created in excited states, their presence can be observed using ultraviolet-visible fluorescence spectroscopy or even through the direct detection of these particles, in the case that they have long lifetimes. Thus, Lyman-α and Balmer radiation from excited H atoms has been observed at the C 1s-to-Rydberg excitations of the methane molecule.[7] Additionally, some of us have recently investigated the neutral fragment production at the C 1s edge of CH_4 by observing coincidences between neutral particles and positive ions.[8] In that work, the neutral particles included both excited H atoms and vacuum ultraviolet (VUV) photons, but no heavier neutral fragments were detected. Some of the excited H atoms were shown to be in rather high Rydberg (HR) states ($n \geq 21$; n is the principal quantum number of the Rydberg orbital) because they could be ionized with an electric field.

The production of neutral HR fragments at a core edge of a molecule was first detected in the N_2 molecule[9] and has later been reported in some other small molecules such as HCl,[10] H_2O,[11] CO,[12] and CO_2.[13] The peaks observed just above the inner-shell ionization potentials have been attributed to recapture processes that occur in the context of

a)Author to whom correspondence should be addressed. Electronic mail: kivimaki@iom.cnr.it

the so-called post-collision interaction (PCI).[14] Classically, a slow photoelectron experiences a change in the field of the molecular ion core (from +1 to +2), when a subsequently emitted faster Auger electron passes it. The two electrons can exchange energy in the field of the ion, as a result of which the photoelectron may even be recaptured to a HR orbital of the molecular ion. The ion thus ends up in a val^{-2}-HR^{1} state. Upon dissociation, the Rydberg electron can be transferred to a HR orbital of a fragment. HR fragments have also been observed at photon energies corresponding to the excitation of inner-shell electrons to unoccupied valence and Rydberg orbitals. Resulting neutral core-excited states usually decay by electron emission, which in this case is called resonant Auger decay. Some resonant Auger transitions can populate final states which generate neutral HR fragments during dissociation.

In the 1980s, high-resolution studies of valence electron transitions experienced significant progress with the development of zero-kinetic energy photoelectron (ZEKE-PE) spectroscopy.[15,16] In the original scheme of ZEKE-PE spectroscopy,[15] the tunable photon energy obtained from a laser system was used to ionize a sample gas in (nearly) field-free conditions and electrons ejected with $E_{kin} \approx 0$ meV could be separated from other electrons with the aid of a delayed pulsed field. The experimental observation of long-lived HR states near ionization thresholds led to the development of another ZEKE detection scheme: pulsed field ionization (PFI) of HR states. HR states converging to the first ionization energy of a molecule have long lifetimes, which are proportional to n^3. An electric field, F, lowers the ionization potential of a species approximately by the amount of $\Delta E = 6\sqrt{F}$, where E is given in cm^{-1} and F in V/cm.[17] When scanning the photon energy, HR states that are separated from the IP by less than ΔE become visible in the ZEKE spectrum measured with PFI. Pulsed fields used in these measurements are small, typically < 1 V/cm. A variant of this technique, mass-analyzed threshold ionization (MATI) spectroscopy,[18] has also been developed. It is closely related to ZEKE-PE spectroscopy, but it detects ions — instead of electrons — produced by pulsed field ionization. These ions can be identified based on their flight times in a time-of-flight (TOF) spectrometer. The main difficulty of MATI spectroscopy consists of detecting only ions produced by PFI of long-lived HR states while avoiding the detection of ions produced directly during the exciting laser pulse.[19] As far as we know, MATI spectroscopy has not been used in studies of inner-shell processes.

In the present study, we have developed an experimental technique that combines PFI with soft x-ray excitation. It allows us to determine which neutral fragments are created in HR states after core excitation processes in molecules. The experiment exploits PFI with high electric fields (of the order of kV/cm). A special feature of our apparatus is that field ionization of HR fragments occurs in a region that is separated from their place of creation. This allows us to perform measurements in the usual multi-bunch operation mode of a synchrotron light source. Here, we present first results obtained at the C 1s edge of the CH_4 molecule and interpret them with the aid of the previous coincidence studies and quantum chemical calculations.

II. EXPERIMENTAL METHOD

The experiments were performed at the Gas Phase Photoemission beam line of the Elettra synchrotron radiation laboratory (Trieste, Italy). The beam line has been described in detail before.[20] Briefly, it uses an undulator as a light source and a spherical grating monochromator for the selection of the photon energy. The photon energy range of the beam line is 13.5-900 eV, and the radiation is linearly polarized. High resolving power ($>10^4$) can be achieved at most energies, thanks to five interchangeable gratings.

The basic idea of the experiment is as follows. The photon beam from the beam line crosses a molecular beam of sample gas in the interaction region. Let us assume that this interaction produces neutral fragments in HR states and that some of them move towards a TOF spectrometer, while positive ions are blocked by a suitable arrangement of potentials. When a HR fragment enters the first stage of the TOF spectrometer, it can be ionized by a pulsed electric field. The voltage pulse, thus, gives a reference time for the formation of a positive ion, created from the HR fragment. The flight time of this ion in the TOF spectrometer allows us to identify the original neutral HR fragment.

In order to measure the flight times of field-ionized species, we have modified the existing Wiley-McLaren TOF spectrometer[21] which has previously been used to detect neutral-particle–photoion coincidences.[8,13] The scheme of the modified experimental setup is shown in Fig. 1. A pulsed field ionization region (P in Fig. 1) was added between the interaction region (I) and acceleration region (A). Region P was kept as short as possible (2 mm), because it acts as a source of ions in the present experiment and its length affects mass resolution. The shape of the electrode between regions P and A was determined by construction requirements; in the following, we call it the "hat" electrode because of its shape. Another modification was the extension of the field-free drift tube from 105 mm to 203 mm in order to achieve a higher mass resolution for field-ionized fragments.

Before construction, numerical simulations using the SIMION software package were performed in order to estimate the potentials of the electrodes of the TOF spectrometer for optimum mass resolution. An iterative script was written for the simulations. The chosen grid potential was changed stepwise, while other potentials were kept fixed. At each step, thousands of ions of chosen masses and kinetic energy distributions were created in the entire field ionization region (P) and their arrival times were recorded at the detector plane. The value of the potential for the experiment was selected based on the resolution of the calculated TOF spectrum. The simulations suggested that the electric fields in regions A and P should have a ratio of ~8.3. This condition is fulfilled when the drift tube is set at −2.5 kV, the hat electrode is at ground, and a voltage pulse with amplitude of +300 V is applied. When the voltage pulse is off, the entrance mesh is at ground potential. Note that the modified TOF spectrometer still operates on the space focusing principles that Wiley and McLaren presented 60 yr ago.[21]

A potential of −100 V was applied to the mesh opposite to the ion TOF spectrometer in order to extract all positive ions

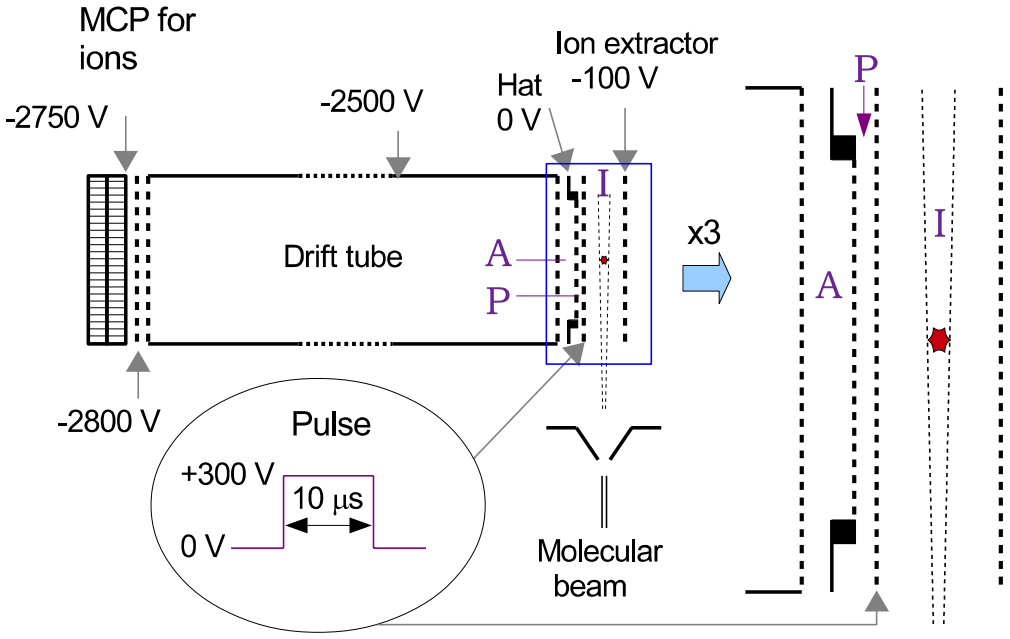

FIG. 1. The scheme of the experimental setup. HR fragments created in the interaction region (I) can enter the time-of-flight spectrometer. A positive pulsed potential (frequency 10 kHz) is applied to the electrode on the left side of interaction region; thus, it can field ionize HR fragments in region P. At the same time, ions created in region I are prevented from entering the instrument. The rising edge of the voltage pulse is used as a start signal for the flight time measurement, while ions hitting the microchannel plate (MCP) detector provide stop pulses. The width of the interaction region is 11 mm, the distance between the pulsed and hat electrodes is 2 mm, and the distance between the hat electrode and the drift tube is 5 mm along the central axis of the TOF spectrometer. The length of the drift tube is 203 mm. The drawing on the right side shows a magnification of regions A, P, and I.

created in the interaction region. Electrons and negative ions were repelled by a high negative potential of the drift tube. In this configuration, only photons and neutral fragments can enter the TOF spectrometer; the latter need to have an initial velocity — obtained in dissociation — directed towards the TOF spectrometer. The electric field in the field ionization region P was about 1.5 kV/cm, which can ionize H(n) atoms with $n \geq 22$ and C atoms below the first IP in the nd states with $n \geq 20$.[22] (C atoms in other nl states can be field ionized as well, but their energies are not given in Ref. 22.) As mentioned above, the rising edges of the pulsed voltage are used as start signal for time-of-flight measurements, while particles detected by the MCP detector of the TOF spectrometer provide stop signals. These signals were fed into a time-to-digital converter system (ATMD-GPX from ACAM Messelectronic GmBH).

Fragments in HR states that are in region P when the high voltage pulse arrives can be field ionized, accelerated towards the detector, and they can create time-correlated events. The MCP detector of the TOF spectrometer can detect other neutral particles (listed below) which do not give rise to peaks in the TOF spectra but contribute to the background. First, HR fragments can be field ionized in the acceleration region (A in Fig. 1), where there is a high static electric field. The resulting positive ions are accelerated towards the MCP detector and detected but are not time-correlated with the start pulses. Second, a typical MCP detector can directly detect neutral long-lived fragments, i.e., without conversion to ions, if their internal energy is higher than about 9 eV. In the present study, neutral fragments in Rydberg states with $n \approx 10$-15 belong to this category. Third, the detector can also detect VUV and soft x-ray photons. Photon emission is not correlated with the voltage pulses, but even if it were, it would lead to a sharp and well-isolated peak in the TOF spectrum. During the experiment, we saw no evidence of any contamination from ions created in region I in the MCP signal, when the potentials indicated in Fig. 1 were applied.

We finally note that by switching off the voltage pulsing we can record a sum of HR fragments, VUV, and soft x-ray photons as a function of photon energy. In such spectra, field ionization of HR fragments occurs in region A, but the resulting ions are not mass analyzed.

Methane used in the experiment was obtained from SIAD S.p.A. with stated purity of 99.95% and was used as delivered. It was introduced into the interaction region (I) as a molecular beam, using a stagnation pressure of 0.2 bars, expanded into vacuum through a 50 μm orifice. The background pressure of the chamber was $\sim 2 \times 10^{-7}$ mbars, rising to 1.6×10^{-6} mbars with the molecular beam on. The molecular beam passes the interaction region without hitting the electrodes of the TOF spectrometer. The incident photon beam was almost circular in shape and had a diameter of about 300 μm. Measuring conditions remained stable during the measurements; in particular, the Elettra storage ring operated in the top-up mode with a practically constant electron current. Field ionization TOF spectra were recorded by repeating scans of 15 or 30 min for total measuring times of several hours. All data were used in the analysis, as they were similar within statistical fluctuations.

III. EXPERIMENTAL RESULTS

The sum of HR fragments and energetic photons was measured by scanning the photon energy across the C 1s

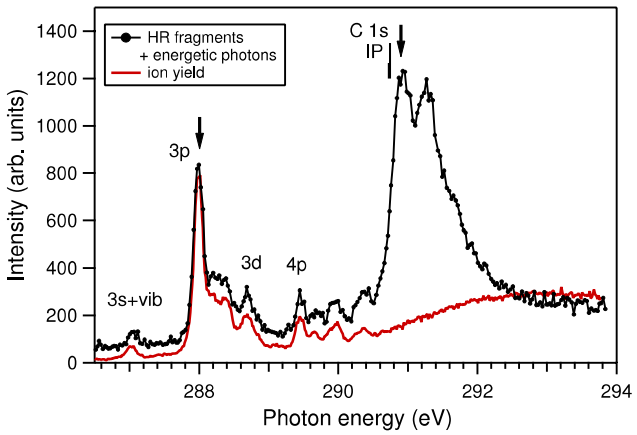

FIG. 2. The spectrum containing the sum of HR fragments, VUV, and soft x-ray photons at the C 1s edge of CH_4 in comparison with the ion yield. The curves have been normalized to the photodiode current and scaled at the 3p resonance. The photon energy resolution was about 120 meV. The arrows indicate the photon energies where the spectra of Fig. 3 were measured.

edge with the entrance mesh of the TOF spectrometer kept at ground and a static electric field of ~5 kV/cm applied in region A (see Fig. 1). In this field, H(n) atoms with n ≥ 16 or so can be ionized.[22] The result obtained with an acquisition time of 10 s/energy point is shown in Fig. 2 (black dots). It is compared to the spectrum measured with the same setup and 1 s/point acquisition time, after changing the potential on the ion extractor mesh from −100 V to −3 V (lighter solid curve in Fig. 2). The potential of −3 V was set in order not to saturate the MCP detector. While the potential of −100 V in the ion extractor prevented all ions from entering the TOF spectrometer, the smaller potential of −3 V allowed some fast ions (with kinetic energy higher than ~1.5 eV) to be detected. In this way, we could measure an ion yield spectrum of methane using the same photon resolution. The intensities of the two curves in Fig. 2 have been scaled to their peak heights at the C 1s → 3p transition located at 288.00 eV.[23] The sum of HR fragments and energetic photons shows a higher background than the ion yield measured with the same detector. This is mostly due to detection of VUV photons (in particular, Lyman emission in H atoms) produced by valence ionization processes and to a small extent also to the longer acquisition time needed to record the spectrum.

The curves in Fig. 2 show the well-known C 1s-to-Rydberg resonances between the photon energies of 287 and ~290.7 eV, see, e.g., Refs. 23 and 24. In the neutral particle spectrum (black curve), an additional, distinct double-peak feature appears around 291 eV, i.e., just above the C 1s IP of 290.735 eV.[24] The curve resembles the H(HR)–H^+ coincidence yield presented in the previous study (Fig. 4 in Ref. 8) but displays higher statistics. The peaks observed just above the C 1s IP arise from HR fragments that are produced when a slow C 1s photoelectron is recaptured after Auger decay, and the resulting molecular ion in a HR state dissociates. The fine structure is due to the vibrational structure of the C $1s^{-1}$ state.[8] Such features were not observed in the Lyman-α or visible photon fluorescence yield spectra recorded at the C 1s edge.[7] To our knowledge, the x-ray fluorescence yield spectrum of methane at the C 1s edge has not been published, but, similarly to the x-ray fluorescence yield spectra of other small molecules,[25] we do not expect strong features appearing just above the core IP. In addition, the x-ray emission intensity at the carbon 1s edge is very weak. Apart from single-hole C 1s ionization, no new resonant or direct ionization channels open in the energy region of 291-293 eV: single core excitations are all located below the C 1s IP, next higher energy resonant transitions are core-valence double excitations located around 303 eV,[4] and there is no shape resonance in the C 1s ionization continuum of methane.[26]

In the following, we estimate the relative importance of the production of HR fragments at the C 1s IP. According to Flammini *et al.*,[6] CH_x^+ ions (x = 0-3) originating from dissociation after Auger decay have average kinetic energies below 1 eV; hence, we can assume that the fast ions detected in the lighter curve of Fig. 2 were predominantly H^+, with only marginal contributions from H_2^+ or heavier ions. The ion yield curve also contains a portion from HR fragments and energetic photons, which were not affected by the change of the potentials in the ion extraction region. The count rate of all HR fragments at the maximum of the black curve was about 100 Hz. In the "fast ion" yield, about 870 counts/s were detected at the same photon energy, including ~100 initially neutral HR fragments. We thus obtain a branching ratio of 11.5% for HR fragments at the C 1s IP. However, we should consider the collection efficiency of H^+ ions. Kinetic energy release distributions have been reported for different fragmentation channels of the doubly charged methane.[6,27] The results of different studies show quite large variations. As an average, we assume for H^+ ions a Gaussian kinetic energy distribution with the maximum at 3.5 eV and full width at half maximum of 3.0 eV. Assuming additionally an isotropic angular distribution, we simulated using the SIMION software package the trajectories of H^+ ions in the TOF spectrometer in the experimental conditions of the "fast ion" yield (the lighter curve in Fig. 2). We calculate a transmission of ~13% for all H^+ ions. More importantly, for comparison with the HR fragment yield, we estimate that about 60% of those H^+ ions that are ejected within the acceptance angle of the TOF spectrometer become detected. Finally, at 300 eV photon energy, 52.6% of all ions are H^+.[2] This very crude estimate suggests that neutral HR fragment production amounts to ~4% of the positive ion yield just above the C 1s IP, a result which is similar to the ~3% found for the intensity ratio between neutral HR fragments and ionic fragments just above the N 1s IP for the N_2 molecule.[9] These numbers indicate that the production of neutral HR fragments is a minor, but not negligible fragmentation channel in photoionization experiments performed just above core IPs. At the C 1s → 3p resonance of CH_4, the branching ratio of all HR fragments drops by one order of magnitude with respect to the one just above the C 1s IP.

TOF spectra of HR fragments created by photoionization of methane molecules were measured using pulsed field ionization at the C 1s → 3p resonance and just above the C 1s IP, where the most intense production of HR fragments was expected based on the black curve in Fig. 2. The spectrum recorded above the C 1s IP is shown in Fig. 3(a); its intensities were obtained by binning the arrival times within 4 ns wide windows. The detection window opened 440 ns after each start

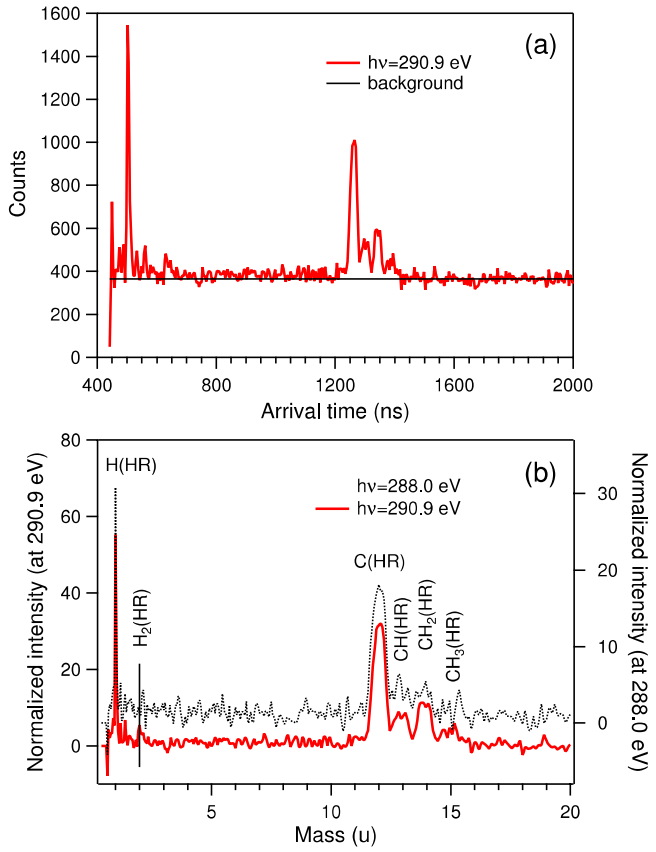

FIG. 3. (a) The solid curve shows the time-of-flight spectrum of field-ionized HR fragments of the CH_4 molecule measured at the photon energy of 290.9 eV (just above the C 1s IP). The black horizontal line shows the constant background subtracted from the spectrum before its conversion to a mass scale. (b) The background-subtracted TOF spectra shown on a mass scale. The measuring times were 6 and 12.5 h at the photon energies of 288.0 and 290.9 eV, respectively. The intensities of the two spectra have been normalized to the photodiode current and measuring time. A vertical line shows the expected position of the H_2(HR) fragment.

signal in order to avoid noise from the high-voltage pulses. Some artifact signals still remain around 500 ns, close to the highest peak of the TOF spectrum. Fig. 3(b) shows the data on a mass scale (after background subtraction), assigning the two most intense peaks to H(HR) and C(HR) atoms. The assignment of the second highest peak to C(HR) was confirmed by similar measurements of the CO_2 molecule.

At the photon energy just above the C 1s IP (lower curve in Fig. 3(b)), we attribute the production of HR fragments to recapture processes and subsequent dissociation of the parent ions. This is in agreement with the earlier studies of the neutral HR fragment production in small molecules, e.g., Refs. 8, 9, and 13. We observe that such processes in methane can yield different HR fragments; in fact, all possible neutral HR fragments appear in the spectrum. (CH_4(HR) molecules are not expected to be detected, since they cannot have a substantial velocity component in the direction perpendicular to the molecular beam.) Their branching ratios, as obtained from a Gaussian fit to the background-subtracted TOF spectrum of Fig. 3(a), are presented in Table I. The H_2(HR) peak is weak but appears exactly in the correct position in the lower spectrum of Fig. 3(b). In contrast, the H_2(HR) peak does not rise above the noise level in the upper spectrum of Fig. 3(b). The error

TABLE I. Branching ratios of the neutral HR fragments at 290.9 eV photon energy (this work), singly charged positive ions created with 300 eV photons[2] (above C 1s edge), and ions observed in coincidence with Auger electrons.[5]

	This work		Reference 2	Reference 5
H(HR)	23^{+1}_{-3}	H^+	52.6	42.9
H_2(HR)	3^{+1}_{-3}	H_2^+	2.3	4.6
C(HR)	42 ± 1	C^+	9.7	11.5
CH(HR)	11 ± 1	CH^+	14.4	16.5
CH_2(HR)	15 ± 1	CH_2^+	15.4	18.7
CH_3 (HR)	7 ± 1	CH_3^+	4.4	5.8
...	...	CH_4^+	1.2	...

limits given in Table I contain a statistical fitting error of ±1%. The total errors in the H(HR) and H_2(HR) intensities are larger because of the noise caused by the high-voltage pulse which appears near the arrival times of the lightest fragments.

The branching ratios of neutral HR fragments observed in the present work (see Table I) are completely different from those of the corresponding ions observed with mass spectroscopy at the photon energy of 300 eV.[2] They also differ from the branching ratios obtained by fitting the Auger electron-photoion coincidence spectrum from Ref. 5 (last column in Table I), where some fast H^+ ions escaped detection. H(HR) fragments have previously been detected in neutral-particle–photoion coincidence experiments,[8] while the CH_4(HR) molecule and molecular CH_x(HR) (x = 1-3) fragments have been detected after 60 eV electron impact on methane.[28]

The field-ionization mass spectrum measured at the C 1s → 3p excitation (Fig. 3(b), upper curve) has worse statistics, making the changes in the relative peak intensities between the resonance and the C 1s threshold uncertain. However, also the spectrum measured at the resonance is clearly dominated by the C(HR) and H(HR) fragments. The normalized intensities of the peaks indicate that the production of HR fragments is about two times more probable just above the C 1s threshold compared to the C 1s → 3p resonance. As the intensity ratio of the peaks is about 1.5 (instead of 2) in Fig. 2, we estimate that VUV and soft x-ray emission contribute with about 25% to the intensity of the C 1s → 3p peak in the sum of HR fragments and energetic photons spectrum. If we take into account the photoabsorption cross section, which is ~10 times larger at the C 1s → 3p resonance than just above the C 1s threshold,[24] we get an order-of-magnitude estimate that, per absorbed incident soft x-ray photon, C 1s photoionization just above the core IP is about 20 times more likely to produce HR fragments than the C 1s → 3p resonant excitation.

The angular distributions of ejected neutral HR fragments influence the results obtained with the present setup. Such effects are, however, expected to be very weak in the present case. Kosugi has reported angle-resolved fragment ion yields at the C 1s edge of methane.[29] Slightly different intensities at 0° and 90° were observed at most excitation energies, but not at the C $1s^{-1}$ → 3p, $\nu = 0$ resonance. Geometric distortion in the core-excited state of the CH_4 molecule through vibronic coupling was shown to be essential for

anisotropic fragmentation. As vibronic coupling does not play a role in the transitions to the vibrationless electronic states C $1s^{-1}$ $3p^1$ and C $1s^{-1}$, we expect that angular effects have not modified the intensity ratios of the HR fragment peaks in the measured field ionization mass spectra (Fig. 3). The situation would be different, for instance, in core-excited linear molecules that are preferentially oriented either parallel or perpendicular to the electric vector of the linearly polarized incident light and keep that orientation until dissociation (in the so-called axial recoil approximation). An instrument that is suitable for the measurement of angle-integrated intensity ratios of HR fragments in any molecules could be constructed by installing a present-type TOF spectrometer at the so-called magic angle (54.7°). Alternatively, a setup of two TOF spectrometers mounted at 0° and 90° could be used, which would allow the determination of the angular asymmetry parameters of neutral HR fragments.

IV. THEORETICAL METHODS AND RESULTS

The *ab initio* calculations performed in this work were based on the following assumptions: neutral fragments with a HR electron (i.e., the HR fragments observed in our experiment) have a molecular ion core with the high-Rydberg electron at a large distance ($\langle r \rangle \propto n^2$) having no effect on bonding in the molecular core (the core ion model used in Ref. 30); molecular dissociation can take place just as if the HR electron were not present. We have also assumed that the energies of the neutral HR fragments CH_x(HR) (x = 0-4), H(HR), and H_2(HR) are similar to the energies of the corresponding ions CH_x^+ (x = 0-4), H^+, and H_2^+.

Core ionization and the following single or double Auger decay will result in the production of CH_4 dications or trications (parent ion), which have not been observed. In the model, the HR electron stays in the vicinity of the parent ion, but in the calculations, the HR electron has been ignored. In order to study energetically possible fragmentation channels after parent ion creation, the energies of the dication (trication) as well as the energies of created ions were calculated at the multiconfigurational second-order perturbation (CASPT2) level of theory with a basis set of valence double zeta accuracy with polarization functions (ANO-L-VDZP) using the Molcas 7 package.[31] The experimental ground state geometry, i.e., tetrahedral symmetry with the C–H bond length of 1.089 Å, was taken as the starting point. Using this geometry, the vertical ionization energies of the parent ion(s) were calculated. For dissociation fragments CH_x^+ (x = 1-3), the geometry was optimized. The resulting geometries are shown in Fig. 4.

The calculated energies of the CH_4 dication and CH_x^+ (x = 0-3) ions with corresponding H-based fragments are summarized in Fig. 4. Energies are given in eV with respect to the calculated vertical double ionization energy (38.65 eV) of the lowest singlet state, ^{1}E. The energies calculated here are slightly lower than those given in Ref. 1, but the ordering of the levels is the same. Vertical triple ionization energy was calculated to be 35.68 eV above the vertical double ionization energy and it is, therefore, well above the energy needed for complete atomization of the methane molecule.

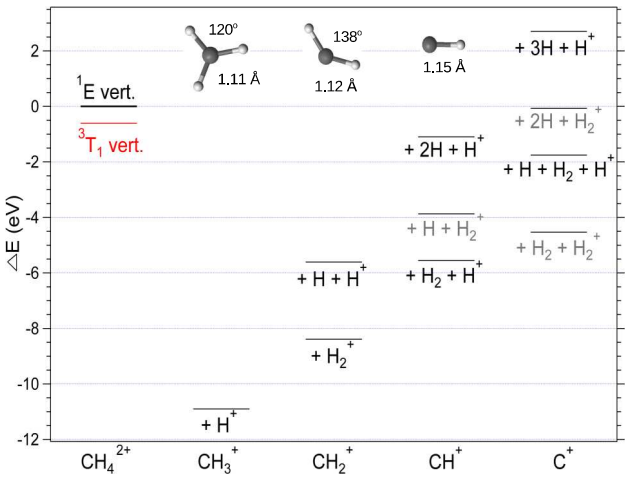

FIG. 4. Energies for different ion pairs after CH_4 dication fragmentation and relaxation. On the left, vertical double ionization energies for the lowest singlet (^{1}E) and triplet ($^3T_1$) states of the CH_4 dication are given. H_2^+ has only been observed in coincidence with CH_2^+ ions;[6,32] hence, other fragmentation channels with H_2^+ are displayed in gray.

The observed HR fragments have long life times and so have many states of the molecular fragment ions calculated in this study. This was investigated by calculating the potential energy curves (PECs) for the ions CH_x^+ (x = 1-3) along one of the C–H bonds at the same level of theory, while optimizing geometry at each bond length. PECs for all three CH_x^+ ions showed a similar behavior with at least one non-dissociative state. In addition, we followed the dynamics of the parent dication/trication on their ground state potential energy surface by following the Minimum Energy Path (MEP), where the geometry of the next step is chosen according to the lowest energy. Our MEP calculations do not take into account the vibrational motion observed in the core ionized state.[33]

V. DISCUSSION

A. Above the C 1s threshold

Very recently, recapture processes to Rydberg states up to n = 15-18 were *directly* observed in a high-resolution photoelectron spectrum of Xe, measured 0.02 eV above the Xe $4d_{5/2}$ photoionization threshold.[34] Even higher Rydberg orbitals were populated, but those transitions formed an unresolved spectral feature. Similar observations do not exist for molecules. Their spectra would be more difficult to interpret because more electronic states are available and vibrations would also complicate the situation. However, the PCI effect is conceptually the same for atoms and molecules, and there is absolutely no reason why recapture processes should not take place in molecules. In fact, they have been used to explain the enhanced production of HR fragments in just-above-threshold core-level photoionization of small molecules,[8–13] as mentioned in the Introduction.

The photoelectron recapture is an ultrafast process which occurs before the dissociation of the molecular ion. More formally, one should treat the photoelectron emission, Auger decay, and photoelectron recapture as a one-step scattering process.[35] It is, therefore, actually incorrect to say that the

photoelectron recapture takes place after the Auger decay. We nevertheless use the two-step picture, because it is conceptually easy to follow and it can explain the major features of the experimental results. HR fragments are thought to arise when molecular ions in HR states dissociate. An electron in a distant HR orbital interacts very weakly with the electrons in valence orbitals; hence, it is not expected to affect how the doubly charged molecular core dissociates after Auger decay. After dissociation, the HR electron can attach, at least in principle, to any ionic fragment, forming also neutral fragments in HR states.

Next we consider what information can be obtained by comparing the ionic fragmentation after Auger decay[5,6] to our field ionization mass spectra of HR fragments. If the recaptured electrons attached with equal probability to any ionic fragment after dissociation, our field-ionized mass spectra of HR fragments would show similar relative intensities as the ion spectra integrated over all the final states of Auger decay. In practice, some fast H^+ ions escaped detection in the coincidence measurements,[5,6] so the relative intensity of H^+ appeared too low in the spectra. The branching ratio of H^+ after Auger decay is probably above 50%, as was found in non-coincidence measurements[2] at the photon energy 300 eV (see the fourth column in Table I), where C 1s single-hole ionization is the most likely process. The relative intensities of the other singly charged ions produced after Auger decay are given in Table I and they increase in the following order: H_2^+, CH_3^+, C^+, CH^+, and CH_2^+.[5] We directly see that the order is not the same as in the field-ionization mass spectrum shown in Fig. 3(b) (lower curve), where the C(HR) peak displays by far the greatest intensity, being almost three times higher than CH_2(HR). The intensities of the molecular fragments CH_x(HR) (x = 1-3) follow the same order in the present work and in Ref. 5, although with somewhat different intensity ratios.

Calculation of potential energy curves of the CH_x^+ (x = 1-3) ions shows that each of these ions can form stable and possibly also metastable states, which is confirmed by their detection in mass spectroscopic studies where flight times are usually in the microsecond range. The calculated PECs of different ions (not shown) do not explain why a particular CH_x(HR) (x = 1-3) fragment should be favored. Here, only a few lowest energy curves should be of importance since higher electronically excited states would either dissociate or autoionize to the continuum of a lower ionic state before detection. Calculated energies depicted in Fig. 4 show that vertical double ionization to the lowest dication states will enable, on purely energetic grounds, fragmentation to all CH_x^+ (x = 0-3) ions. According to these energies, two-step processes suggested by Flammini *et al.*[6] should occur via intermediate CH_3^+ ions having considerable internal energy, since it is not energetically possible for the relaxed CH_3^+ ion in the ground state to fragment further.

Kukk *et al.*[5] found that the production of the CH_3^+ ion seems to be uniquely correlated with the population of the $1t_2^{-2}$ (^1E) final state in Auger decay. In other words, $CH_4^{2+} \rightarrow CH_3^+ + H^+$ dissociation is not observed to occur after any other Auger transitions. If this is true, when the CH_4^{2+} ion in this particular electronic state recaptures the photoelectron in a HR orbital, subsequent dissociation should be the only channel that produces CH_3(HR) fragments. Similarly, the fragmentation $CH_4^{2+} \rightarrow CH_2^+ + H_2^+$ only takes place after Auger decay to the $1t_2^{-2}$ ($^1T_2$) final states.[5] This is also supported by results in Refs. 6 and 32, where H_2^+ was detected in coincidence with CH_2^+ ions only. If the CH_4^{2+} in this final state recaptures the C 1s photoelectron, the subsequent dissociation provides the predominant channel to obtain H_2(HR) fragments. The observation of the CH_3(HR) and H_2(HR) fragments indicates that in the dissociation of the CH_4^+(HR) ions, either a heavy or light fragment can retain the electron in the HR orbital. For energetically higher final states of Auger decay, second step dissociation channels are open and higher internal energy of the ion can lead to further fragmentation.

Thus, the presence of the CH_3(HR) fragment strongly implies that some of the observed HR fragments are produced after single Auger decay, when the slow C 1s electron is recaptured. If CH_3(HR) acts as an intermediate, as suggested by Flammini *et al.*,[6] this could explain the reduced intensity ratios of the CH(HR) and CH_2(HR) fragments when compared with the corresponding ions after Auger decay (Table I). This could be rationalized if in the subsequent dissociation step the electron in the HR orbital can be transferred to either a CH_x^+ ion or to a proton. However, this scheme of sequential dissociations after Auger decay does not explain the large intensity of the C(HR) peak in our spectrum (Fig. 3) and thus the single Auger decay cannot be the only source of HR fragments.

We note that the relative intensity of the C^+ ion created after Auger decay surpasses those of CH^+ and CH_2^+ if one considers Auger decay to the final states $2a_1^{-2}$ and it still increases when going to lower kinetic energies (or higher binding energies).[5] The final states located in that lowest kinetic energy part of the Auger spectrum have general electron configurations of type $(2a_1 1t_2)^{-3}$ $virt^1$ and they arise from correlation effects.[36] The calculated energy for vertical triple ionization is 35.68 eV above the vertical double ionization threshold, so a second-step (participator) Auger decay is possible for higher electronic states of CH_4^{2+}, which would lead to emission of slow electrons and the creation of triply charged states of CH_4. C 1s ionization in methane initiates a symmetric stretch vibrational mode and this nuclear motion continues after Auger decay. Our MEP calculations for both the dication and trication ground states did not account for any initial motion of the nuclei. Nonetheless, according to our calculations, direct double/triple ionization from the neutral ground state resulted in lengthening of all bonds before the charge localization and resulting charge separation. For higher electronic states, the greater internal energy available for nuclear dynamics (most probably initiated already in the core-ionized state) results in a more complete fragmentation even if the proton left the parent ion slightly before neutral hydrogen atoms.

Triple ionized states can also be reached in double Auger transitions, where two electrons are emitted simultaneously. In that case, they can share the available energy in a continuous manner. Using a magnetic bottle time-of-flight spectrometer, Eland *et al.*[37] have studied processes that lead to triple ionization of methane after the removal of a C 1s electron.

They determined that the energies of the triply ionized states begin from ~67 eV above the ground state of the CH_4 molecule and they form clear maxima around 76.4 (±0.2) eV for the $1t_2^{-3}$ states and 86.2 (±0.2) eV for the $2a_1^{-1}\,1t_2^{-2}$ states. Taking into account the C 1s IP of 290.375 eV,[24] spectral intensity due to double Auger decay is then located below the kinetic energy of 223 eV. The relative ion yields of Ref. 5 did not extend to such low kinetic energies, but one could extrapolate that — within the series CH_x^+ (x = 0-3) — the C^+ ion is the most probable dissociation product following double Auger decay. A study of multiply ionized methane created in collisions with swift Xe^{21+} ions also indicates that CH_4^{3+} most likely fragments to $C^+ + H^+ + H^+ + 2H$.[38] Eland *et al.*[37] determined that the energy distributions of electrons resulting from emission of two Auger electrons display increased intensity towards zero kinetic energy. The intensity ratio of triple ionization (double Auger) to double ionization (normal Auger) was found to be approximately 0.035:1 at 296 eV.

We believe that double Auger decay is mainly responsible for the large intensity of C(HR) fragments in our field-ionization spectrum measured above the C 1s IP. Sheinerman *et al.*[39] have studied experimentally and theoretically the post-collision interaction effect in the context of double Auger decay from the $2p^{-1}$ states of Ar. They found that the PCI distortion of the photoelectron line profile is clearly larger for double Auger decay than for single Auger decay, if the photoelectron is slower than both the Auger electrons (see Fig. 3 in Ref. 39). This is because the ionic field experienced by the photoelectron changes by two charge units in such double Auger decay, Z: +1 → +3. The larger energy shift towards lower kinetic energies and the larger width of the photoelectron line also imply, in our opinion, that recapture of the photoelectron becomes more likely in double Auger decay than in single Auger decay. On the other hand, there is not much difference in PCI distortion between the double and single Auger decay, if the photoelectron is faster than one of the Auger electrons emitted in double Auger decay.[39] A similar result was also obtained when the second Auger electron is emitted sequentially (in Auger cascade).

We can illustrate the suggested pathway to the production of C(HR) fragments by writing the intermediate steps in the context of double Auger decay,

$$\begin{aligned}
CH_4 + h\nu &\rightarrow CH_4^+(C\ 1s^{-1}) + e_{ph} && \text{(C 1s ionization)}\\
&\rightarrow CH_4^{3+}(Val^{-3}) + e_{ph} + e_{A1} + e_{A2} && \text{(double Auger decay)}\\
&\rightarrow CH_4^{2+}(Val^{-3}\text{-HR}) + e_{A1} + e_{A2} && \text{(recapture to HR orbital)}\\
&\rightarrow C(HR) + 2H^+ + 2H + e_{A1} + e_{A2} && \text{(dissociation).}
\end{aligned}$$

Here, e_{ph} is a C 1s photoelectron and e_{A1}, e_{A2} are two Auger electrons. The protons and H atoms in the last step could, in principle, also appear as molecular species (H_2, H_2^+); however, H_2^+ has not been observed in coincidence with C^+.[6,32] Dissociation in the last step could also produce H(HR) fragments, but C(HR) seems to be the preferred outcome. A reason for this could be that the overlap of the wavefunctions of the occupied HR orbital before dissociation (i.e., in the $CH_4^{2+}(Val^{-3}\text{-HR})$ ion) and after dissociation (in C(HR) or H(HR)) should be larger, when a C(HR) fragment rather than a H(HR) fragment is formed. This can be expressed in another way: a HR orbital of C(HR) should be very similar to the corresponding HR orbital of CH_4^{2+}(HR), since the latter is also built around the central C atom, and this should favor the formation of C(HR) fragments after recapture processes in the context of double Auger decay.

B. At the C 1s → 3p resonance

The intensity of HR fragments is surprisingly high at the C 1s → 3p resonance, considering that the well-established mechanism for their production — recapture following core photoelectron emission — cannot play a role here because no photoelectron is emitted. Thus, there must be other processes that populate HR states of CH_4^+ and CH_4^{2+} ions, which upon dissociation yield HR fragments. The simplest processes that can create CH_4^+(HR) ions at the C 1s → 3p resonance are shake-up transitions during resonant Auger decay: when a resonant Auger electron is emitted, the spectator electron in the 3p orbital may shake up simultaneously to a higher np orbital. Armen[40] has calculated shake-up and shake-off probabilities for an electron in a hydrogenic nl orbital in light atoms, when the (apparent) central charge suddenly changes from Z to Z + 1. He found that the probability $P_{n,m}$ for an nl → ml shake-up transition approaches m^{-3}, when $m \gg n$. In the present experiments, m is of the order of 20-30 (for the HR fragments), so $P_{n,m}$ would be in the range of 10^{-5}-10^{-4}.

Another mechanism that could produce CH_4^+(HR) ions is resonant double Auger decay (or resonant Auger shake-off decay, a term used in Ref. 41) followed by electron recapture. If two electrons are emitted in a resonant double Auger process, their kinetic energy distribution may follow the pattern of asymmetric energy sharing observed in double Auger decay of Ar atoms:[42] one electron tends to retain most of the available energy while the other electron is slow. Hints of such a trend were observed also in methane.[37] The situation resembles that in recapture processes above core ionization threshold: a fast electron and a slow electron are in the vicinity of a doubly charged molecular core, whereby the slow electron could be recaptured in a Rydberg orbital of the molecular ion. Armen[40] calculated for light atoms that the recapture probability can be quite large for an electron in the continuum; it can, in

fact, be much larger than the shake-off probability in resonant Auger decay. Since the latter was predicted to be in the range of 10^{-3}-10^{-2} for Z = 5 (and by extrapolation also for carbon, Z = 6), a slow electron emitted in resonant double Auger decay may produce HR states of the parent ion more efficiently than shake-up transitions during usual resonant Auger decay. The two channels cannot be resolved experimentally, and their division may not even be conceptually necessary.

We may also consider sequential emission of two electrons in the de-excitation of a core-excited state. These processes happen when the final state of the first-step resonant Auger decay is so highly excited that it can decay further by emitting a second electron. However, in this scenario, the first emitted resonant Auger electron is fast; hence, the second emitted electron cannot overtake it. Even if the lifetime of the valence excited state were in the femtosecond range, it is questionable whether the two electrons can exchange energy so that the slower electron could be recaptured.

As in the case of core-ionization just above threshold, the production of CH_4^+(HR) ions is not sufficient to explain the large intensity of the C(HR) peak at the C 1s → 3p resonance (Fig. 3(b)). According to our energy-level calculations, some of the $2a_1^{-2}\,1t_2^{-1}$ nl final states of resonant double Auger decay are located above the lowest triple ionization threshold, but second-step Auger decay to the corresponding $1t_2^{-3}$ states is not expected to occur; hence, CH_4^{2+}(HR) ions may not be produced in this way. In the isoelectronic Ne atom, Ne^{3+} ions have been observed at the 1s → 3p resonance.[41] They were attributed to direct emission of three electrons, $Ne(1s^{-1}\,3p^1) \rightarrow Ne^{3+} + 3e^-$, since there are no suitable intermediate states available for these ions to be produced in sequential Auger transitions. The branching ratio of that channel, which could be called resonant triple Auger decay, was ~3% of all resonant Auger channels. This value is surprisingly large. Coincidence measurements between Ne^{3+} ions and threshold electrons[41] showed that these ions can be produced together with very slow electrons. Similar processes should happen also in methane, even though likely with a lower probability. We, therefore, expect that the decay $CH_4(C\,1s^{-1}\,3p^1) \rightarrow CH_4^{3+} + 3e^-$ occurs and that some of the emitted electrons have very low kinetic energies. The recapture of the slowest Auger electron in a HR orbital would lead to the creation of CH_4^{2+}(HR) ions. We can also consider that the CH_4^{2+}(HR) ions may be directly created in resonant Auger decay processes. There should be no sharp step in the energy distribution of the complete system, composed of the molecular ion and three electrons, above and below any ionization potential. Therefore, we can imagine that for Auger transitions $CH_4(C\,1s^{-1}\,3p^1) \rightarrow CH_4^{3+} + 3e^-$ with one very slow electron, there are also such transitions where the third electron does not make it into the continuum but ends up in a HR orbital of the CH_4^{2+} ion. When created by this or any other mechanism at the C 1s → 3p resonance, the dissociation of CH_4^{2+}(HR) ions mostly yields C(HR) fragments.

VI. CONCLUSION

We have observed HR fragments at the C 1s edge of the methane molecule by exploiting pulsed field ionization. The sum of the yields of HR fragments and VUV and soft x-ray photons shows all core-to-Rydberg excitations, but only HR fragments contribute to the most intense features that appear just above the C 1s IP. The pulsed-field ionization mass spectrum measured at the C 1s threshold revealed that the HR fragment signal is composed of all possible neutral species: CH_3(HR), CH_2(HR), CH(HR), C(HR), H_2(HR), and H(HR), among which the atomic fragments display the highest intensities. The production of HR fragments is attributed to dissociation of CH_4^+ and CH_4^{2+} ions in HR states. At the C 1s threshold, such ionic states can be populated by recapture processes, in which the slow photoelectron loses energy and returns to a HR orbital of the molecular ion, while the fast Auger electron gets even more kinetic energy. The large intensity of the C(HR) fragments can be explained by recapture processes occurring in the context of double Auger decay. Even though double Auger decay is far less likely than single Auger decay, the higher recapture probability of the slow photoelectron after double Auger decay enhances the contribution of this decay channel in the production of HR fragments. However, CH_3(HR) and H_2(HR) should mostly be created in recapture processes after single Auger decay.

The field-ionization mass spectrum measured at the C 1s → 3p resonance appears similar to the spectrum taken above the C 1s threshold. We, therefore, suggest that the same CH_4^+(HR) and CH_4^{2+}(HR) states are responsible for the production of the HR fragments both at the C 1s → 3p resonance and just above the C 1s ionization threshold. The probability for the production is considerably smaller, by a factor of ~20, at the C 1s → 3p resonance. The HR fragment production at the resonance may follow direct resonant multiple Auger transitions to the CH_4^+(HR) and CH_4^{2+}(HR) states, which subsequently dissociate. Alternatively, one may consider that such ionic states become populated, when the slowest of two or three Auger electrons emitted in resonant double or triple Auger decay, respectively, is recaptured by the molecular ion. The experimental method described in this work can also be used in valence ionization studies.

ACKNOWLEDGMENTS

We are grateful to A. Stolfa for the construction of new pieces for the ion TOF spectrometer and to E. Kukk for providing us with the coincidence ion data from Ref. 5. We thank K. C. Prince for critical reading of the manuscript. A.S. acknowledges funding from the Swedish Research Council and from the Academy of Finland's Research Council for Natural Sciences and Engineering. J.A.K. acknowledges funding from the Finnish Academy of Science and Letters and from the Vilho, Yrjö, and Kalle Väisälä Foundation. The research leading to these results has received funding from the European Community's Seventh Framework Programme (No. FP7/2007-2013) under Grant Agreement No. 312284.

[1]G. Dujardin, D. Winkoun, and S. Leach, Phys. Rev. A **31**, 3027 (1985).
[2]W. Wolff, L. Sigaud, E. C. Montenegro, V. L. B. de Jesus, R. L. Cavasso Filho, S. Pilling, and A. C. F. Santos, J. Phys. Chem. A **117**, 56 (2012), and references therein.
[3]K. Ueda, M. Okunishi, H. Chiba, Y. Shimizu, K. Ohmori, Y. Sato, E. Shigemasa, and N. Kosugi, Chem. Phys. Lett. **236**, 311 (1995).

[4]A. Kivimäki, M. Neeb, B. Kempgens, H. M. Köppe, and A. M. Bradshaw, J. Phys. B: At., Mol. Opt. Phys. **29**, 2701 (1996).
[5]E. Kukk, G. Prümper, R. Sankari, M. Hoshino, C. Makochekanwa, M. Kitajima, H. Tanaka, H. Yoshida, Y. Tamenori, E. Rachlew, and K. Ueda, J. Phys. B: At., Mol. Opt. Phys. **40**, 3677 (2007).
[6]R. Flammini, M. Satta, E. Fainelli, G. Alberti, F. Maracci, and L. Avaldi, New J. Phys. **11**, 083006 (2009).
[7]K. Jakubowska, G. Vall-llosera, A. Kivimäki, M. Coreno, E. Melero Garcia, M. Stankiewicz, and E. Rachlew, J. Phys. B: At., Mol. Opt. Phys. **40**, 1489 (2007).
[8]A. Kivimäki, J. Álvarez-Ruiz, R. Sergo, and R. Richter, Phys. Rev. A **88**, 043412 (2013).
[9]Y. Hikosaka, P. Lablanquie, and E. Shigemasa, J. Phys. B: At., Mol. Opt. Phys. **38**, 3597 (2005).
[10]Y. Hikosaka, T. Kaneyasu, and E. Shigemasa, J. Korean Phys. Soc. **53**, 3798 (2008).
[11]J. R. Harries, T. Gejo, K. Honma, M. Kuniwake, J. P. Sullivan, M. Lebech, and Y. Azuma, J. Phys. B: At., Mol. Opt. Phys. **44**, 095101 (2011).
[12]T. Gejo, T. Tamura, K. Honma, E. Shigemasa, Y. Hikosaka, and Y. Tamenori, J. Chem. Phys. **136**, 054201 (2012).
[13]A. Kivimäki, M. Alagia, and R. Richter, J. Phys. B: At., Mol. Opt. Phys. **47**, 155101 (2014).
[14]M. Yu, S. A. Kuchiev, and Sheinerman, Sov. Phys. Usp. **32**, 569 (1989).
[15]K. Müller-Dethlefs, M. Sander, and E. W. Schlag, Chem. Phys. Lett. **112**, 291 (1984).
[16]K. Müller-Dethlefs and E. W. Schlag, Annu. Rev. Phys. Chem. **42**, 109 (1991).
[17]F. Merkt, A. Osterwalder, R. Seiler, R. Signorell, H. Palm, H. Schitz, and R. Gunzinger, J. Phys. B: At., Mol. Opt. Phys. **31**, 1705 (1998).
[18]L. Zhu and P. Johnson, J. Chem. Phys. **94**, 5769 (1991).
[19]F. Merkt, Annu. Rev. Phys. Chem. **48**, 675 (1997).
[20]K. C. Prince *et al.*, J. Synchrotron Radiat. **5**, 565 (1998).
[21]W. C. Wiley and I. H. McLaren, Rev. Sci. Instrum. **26**, 1150 (1955).
[22]A. Kramida, Yu. Ralchenko, J. Reader, and NIST ASD Team, NIST Atomic Spectra Database version 5.2, National Institute of Standards and Technology, Gaithersburg, MD, 2014, available at http://physics.nist.gov/asd.
[23]M. Tronc, G. C. King, R. C. Bradford, and F. H. Read, J. Phys. B: At., Mol. Opt. Phys. **9**, L555 (1976).
[24]M. de Simone, M. Coreno, M. Alagia, R. Richter, and K. C. Prince, J. Phys. B: At., Mol. Opt. Phys. **35**, 61 (2002).
[25]M. Alagia *et al.*, Phys. Rev. A **71**, 012506 (2005).
[26]H. M. Köppe, B. S. Itchkawitz, A. L. D. Kilcoyne, J. Feldhaus, B. Kempgens, A. Kivimäki, M. Neeb, and A. M. Bradshaw, Phys. Rev. A **53**, 4120 (1996).
[27]B. Wei, Y. Zhang, X. Wang, D. Lu, G. C. Lu, B. H. Zhang, Y. J. Tang, R. Hutton, and Y. Zhou, J. Chem. Phys. **140**, 124303 (2014), and references therein.
[28]K. Furuya, K. Ishikawa, and T. Ogawa, Chem. Phys. Lett. **319**, 335 (2000).
[29]N. Kosugi, J. Electron Spectrosc. Relat. Phenom. **79**, 351 (1996).
[30]R. S. Freund, S. M. Tarr, and J. A. Schiavone, J. Chem. Phys. **79**, 213 (1983).
[31]F. Aquilante, L. De Vico, N. Ferré, G. Ghigo, P.-Å. Malmqvist, P. Neogrády, T. B. Pedersen, M. Pitonak, M. Reiher, B. O. Roos, L. Serrano-Andrés, M. Urban, V. Veryazov, and R. Lindh, J. Comput. Chem. **31**, 224 (2010).
[32]E. Fainelli, G. Alberti, R. Flammini, F. Maracci, P. Bolognesi, M. Mastropietro, and L. Avaldi, J. Electron Spectrosc. Relat. Phenom. **161**, 51 (2007).
[33]T. X. Carroll, N. Berrah, J. Bozek, J. Hahne, E. Kukk, L. J. Saethre, and T. D. Thomas, Phys. Rev. A **59**, 3386 (1999).
[34]S. Kosugi, M. Iizawa, Y. Kawarai, Y. Kuriyama, A. L. D. Kilcoyne, F. Koike, N. Kuze, D. S. Slaughter, and Y. Azuma, J. Phys. B: At., Mol. Opt. Phys. **48**, 115003 (2015).
[35]H. Aksela, M. Kivilompolo, E. Nõmmiste, and S. Aksela, Phys. Rev. Lett. **79**, 4970 (1997).
[36]O. M. Kvalheim, Chem. Phys. Lett. **86**, 159 (1982).
[37]J. H. D. Eland, P. Linusson, L. Hedin, E. Andersson, J.-E. Rubensson, and R. Feifel, Chem. Phys. Lett. **485**, 21 (2010).
[38]B. Siegmann, U. Werner, and R. Mann, Nucl. Instrum. Methods Phys. Res., Sect. B **233**, 182 (2005).
[39]S. Sheinerman, P. Lablanquie, F. Penent, Y. Hikosaka, T. Kaneyasu, E. Shigemasa, and K. Ito, J. Phys. B: At., Mol. Opt. Phys. **43**, 115001 (2010).
[40]G. B. Armen, J. Phys. B: At., Mol. Opt. Phys. **29**, 677 (1996).
[41]T. Hayaishi, E. Murakami, Y. Morioka, E. Shigemasa, A. Yagishita, and F. Koike, J. Phys. B: At., Mol. Opt. Phys. **28**, 1411 (1995).
[42]J. Viefhaus, S. Cvejanović, B. Langer, T. Lischke, G. Prümper, D. Rolles, A. V. Golovin, A. N. Grum-Grzhimailo, N. Kabachnik, and U. Becker, Phys Rev Lett **92**, 083001 (2004).